Phase Behavior and Microstructure of Microemulsions Containing the Hydrophobic Ionic Liquid 1-Butyl-3-methylimidazolium Hexafluorophosphate

Nishat Anjum,[†] Marie-Alice Guedeau-Boudeville,[†] Cosima Stubenrauch,[‡] and Ahmed Mourchid*,[†]

Matière et Systèmes Complexes (MSC), UMR 7057 CNRS and Université Paris Diderot, 75205 Paris cedex 13, France and School of Chemical and Bioprocess Engineering, University College Dublin, Belfield, Dublin 4, Ireland

Received: September 30, 2008; Revised Manuscript Received: November 3, 2008

The phase behavior and microstructure of the ternary system water/1-butyl-3-methylimidazolium hexafluorophosphate (bmimPF_6)/Triton X-100 was studied as a function of temperature and ionic liquid (IL) mass fraction α. In the present study, a hydrophobic IL instead of commonly used organic solvents such as *n*-alkanes is used. The fish-shaped region is distorted at low and high values of α, whereas it is symmetric at intermediate α. With increasing α, the extension of the three-phase region decreases regarding the surfactant concentration range, whereas it increases regarding the temperature range. For comparison the phase behavior of two ternary water/bmimPF_6/alkyl oligoethyleneoxide (C_iE_j) systems has been investigated. Our results are compared with those obtained for water/*n*-alkane/C_iE_j and IL/*n*-alkane/C_iE_j systems, respectively.

Introduction

Room temperature ionic liquids (RTILs) are believed to be environmentally friendly, nontoxic green solvents having a melting point below room temperature, which is the reason why they have attracted a good deal of attention.[1] Notably, RTILs that are based on the *N*-alkylimidazolium cation have great potential as substitutes for conventional organic solvents in various chemical syntheses.[2,3] RTILs have many advantageous properties, such as near-zero vapor pressure under ambient conditions and nonvolatility at elevated temperature, nonflammability, and thermal stability (300 °C or more); thus, sometimes they are termed environmentally safe.[4] They can potentially be used in a variety of applications such as in electrochemical devices,[5,6] photochemistry,[7] separation processes,[8] and for the preparation of nanomaterials.[9] They also possess the ability to dissolve a wide range of inorganic, organic, and polymeric materials at high concentrations.[3,10] Another interesting aspect of these RTILs is that their physical and chemical properties can be easily tuned by an appropriate selection of cation and anion.[11,12] For example, 1-butyl-3-methylimidazolium tetrafluoroborate (bmimBF_4) is miscible with water, whereas 1-butyl-3-methylimidazolium hexafluorophosphate (bmimPF_6) is immiscible with water. Moreover, the length of the alkyl groups incorporated into the cation can be modified, which again changes their properties in a systematic and controlled way. Thus, RTILs can be used as the hydrophilic or the hydrophobic phase, which automatically leads to their use as solvents in microemulsions (μE).[13−17]

Microemulsions are optically transparent, isotropic, thermodynamically stable solution mixtures of at least three components, namely, two immiscible solvents and a surfactant. The surfactant (sometimes in combination with a cosurfactant) separates the two solvents by forming a monolayer at the liquid−liquid interface. Kahlweit, Strey, and co-workers have performed numerous systematic experiments aimed at generalizing the behavior of μE.[18−21] In a recent review, the general pattern of the phase behavior, properties, and microstructure of μE are summarized.[22] Usually, the polar phase is water (or brine), and the apolar phase is an organic solvent (very often *n*-alkanes are used). However, due to environmental hazards, researchers are trying to find alternatives for organic solvents. Recently, RTILs have been successfully used either to replace water or organic solvents in μE.

Gao et al. have used bmimBF_4 instead of water to prepare nonaqueous bmimBF_4/benzene/Triton X-100 (TX-100)[13] and bmimBF_4/cyclohexane/TX-100[17] μE. They studied the phase behavior of ionic liquid-in-oil (IL/O) μE and found properties similar to those of classical water-in-oil (W/O) μE.[13] The microstructure of IL/O μE has been confirmed by neutron scattering,[15] freeze-fracture electron microscopy,[17] dynamic light scattering, UV−vis, FTIR and ^{1}H NMR spectroscopy.[13] Recently, a detailed phase diagram study of ternary ethylammonium nitrate (EAN)/*n*-alkane/alkyl oligoethyleneoxide surfactant (C_iE_j) systems has been published.[16] The authors investigated the influence of the oil chain length and of the surfactant structure on the efficiency of the μE.

Hydrophobic ILs such as bmimPF_6 have also been used to replace typical organic solvents in ternary water/oil/surfactant systems.[14,23,24] Gao et al. prepared and characterized water/bmimPF_6/TX-100[14] as well as water/bmimPF_6/Tween-20 μE.[25] For the former system they identified three kinds of microstructures, namely, water-in-bmimPF_6 droplets, bicontinuous structures, and bmimPF_6-in-water droplets by using cyclic voltammetry at 25 °C.[14] In recent studies, Seth et al. have also prepared water/bmimPF_6/TX-100 μE and studied the interaction of bmimPF_6 with water.[23,24]

However, apart from ref 16, the above studies have been performed at room temperature (RT), so detailed knowledge about the phase diagram and the structure has not been gained yet. What is completely lacking is a study in which the ratio of the two solvents as well as the temperature is systematically varied. To fill this gap we studied the phase behavior and the

* Corresponding author. E-mail: ahmed.mourchid@univ-paris-diderot.fr.
[†] Matière et Systèmes Complexes.
[‡] University College Dublin.

10.1021/jp808643s CCC: $40.75
Published on Web 12/10/2008

microstructure of ternary water/bmimPF$_6$/TX-100 μE as a function of the temperature (T) and the surfactant mass fraction at different IL mass fractions.

The formation of 1, 2, and 3 phases, the location of the $\tilde{X}$ point (point of highest efficiency $\tilde{\gamma}$ at temperature $\tilde{T}$) and the formation of liquid crystalline phases were determined by optical inspection and polarizing microscopy. In addition, the microstructure of some selected samples was studied by small angle neutron scattering (SANS). Last but not least, we studied the phase behavior of the two ternary systems water/bmimPF$_6$/$C_{12}E_6$ and water/bmimPF$_6$/$C_{14}E_4$. The results are compared with those obtained by others for water/n-alkane/C_iE_j and IL/n-alkane/C_iE_j systems, respectively.

Materials and Methods

1-Butyl-3-methylimidazolium chloride, anhydrous magnesium sulfate, potassium hexafluorophosphate, Triton X-100, dichloromethane, and deuterated water were purchased from Sigma-Aldrich (France). TX-100 is a nonionic surfactant that has a 4-(1,1,3,3-tetramethylbutyl)-phenyl group as hydrophobic part and a oligoethylene oxide headgroup with an average of 9.5 ethylene oxide units. Two different alkyl oligoethyleneoxide nonionic surfactants, namely, $C_{12}E_6$ and $C_{14}E_4$, were purchased from Nikko Chemicals, Japan. All chemicals were molecular grade and were used without further purification. Deionized water was filtered on a 0.25 μm nylon filter and was used to prepare the hydrogenated samples.

IL bmimPF$_6$ was synthesized according to the procedure described by DuPont et al.[26] Briefly, a 1 L round-bottom flask was charged with 1-butyl-3-methylimidazolium chloride (0.37 mol) and potassium hexafluorophosphate (0.37 mol) in 70 mL of water. After being stirred for 2 h at room temperature, chloride ions were replaced by hexafluorophosphate ions. The organic phase was washed three times with water. A 100 mL portion of dichloromethane and 35 g of anhydrous magnesium sulfate were added to the washed organic phase, followed by the filtration and removal of the organic solvent by distillation at 40 °C, resulting in 0.27 mol of bmimPF$_6$.

Microemulsions were prepared by weighing in known amounts of water, bmimPF$_6$, and surfactant in a 2 mL vial. The sealed vials were placed in a transparent water bath. The number of phases (1, 2, or 3) was determined by visual inspection of phase boundaries at temperatures ranging from 25 to 90 °C. The sample compositions of the ternary mixtures are given as the mass fraction of IL in the solvent mixture

$$\alpha = \frac{m_{\mathrm{bmimPF_6}}}{m_{\mathrm{bmimPF_6}} + m_{\mathrm{H_2O}}} \quad (1)$$

and as mass fraction of surfactant in the total mixture

$$\gamma = \frac{m_{\mathrm{surfactant}}}{m_{\mathrm{H_2O}} + m_{\mathrm{bmimPF_6}} + m_{\mathrm{surfactant}}} \quad (2)$$

The samples for optical microscopy were prepared by filling either flat capillaries or closed round cell (0.5 mm path length) from 1-phase-forming samples. The capillaries were flame-sealed. These samples were placed in a controlled heating stage on the optical microscopes equipped with crossed polarizers, (Leitz Wetzlar, Germany and Eclipse TE 300 Nikon, Japan) for equilibration. Temperature-induced phase changes typically occurred in a few minutes, whereas equilibration of the samples in the 2 mL vials took between a few hours and one day.

For SANS measurements, H_2O was replaced by D_2O, which leads to the required contrast between the deuterated polar phase and the hydrogenated ionic liquid. Measurements were carried out at CNRS-CEA joint Léon Brillouin Laboratory, LLB, located in Saclay, France, on PAXY beamline. Two beamline configurations were chosen to cover scattering vectors (q) between 0.02 and 0.6 Å^{-1} by setting the incident neutron wavelength to 6 and 3.5 Å and the area detector to a distance of 2 and 1 m from the sample, in the first and second configuration, respectively. The samples, in sealed quartz cells with a path length of 1 mm, were preliminarily equilibrated at the desired temperature in an oven, overnight, before being transferred to the cell holder preset to the same temperature, namely 31 and 69 °C. The SANS intensities were collected on 1-phase microemulsions with surfactant mass fractions (γ) between 0.5 and 0.7 and IL mass fractions (α) of 0.37, 0.58, and 0.65. An empty quartz cell was used to quantify the background scattering and was subtracted off from the data. The spectra were further normalized by incoherent scattering of H_2O in a 1 mm quartz cell, with the empty cell scattering subtracted off. The resulting data were integrated over the azimuthal angle, because the 2D scattering patterns were isotropic. Both beamline configurations yielded overlapping data without scale adjustment. The scattering intensities, which were also corrected for incoherent scattering estimated from the signal at high q, were subsequently obtained in absolute scale (cm^{-1}).

Results and Discussion

Figure 1 shows phase diagrams of the ternary system water/bmimPF$_6$/TX-100, which were measured as a function of γ and T at six different values of α. The fish-shaped diagrams are constructed on the basis of temperature scans performed at different γ. For γ values below ~0.5 and at low temperature, an IL/W droplet μE coexists (upper phase) with an IL excess (lower) phase ($\bar{2}$ or Winsor I system). At intermediate temperature, a bicontinuous μE coexists with an IL excess phase and a water excess phase (3 or Winsor III). At high temperature, a W/IL droplet μE coexists with a water excess phase ($\underline{2}$ or Winsor II system). At γ values above ~0.5, an isotropic, optically transparent 1-phase μE is observed from low to high temperature (1 or Winsor IV). A comparison of these phase sequences with that of a classical water/n-alkane/C_iE_j system[22] reveals that they are similar. As is the case in the classical systems, the affinity of the hydrophilic headgroup of TX-100 surfactant toward water decreases with increasing temperature due to the dehydration of the ethylene oxide units. This dehydration simultaneously leads to a decrease of the average headgroup area and thus to a decrease of the curvature H of the interfacial layer from positive (IL/W droplets) to negative (W/IL droplets) values via a zero mean curvature (bicontinuous phase). The only difference with classical water/n-alkane/C_iE_j μE is the density of the IL (1.37 g/cm^3), which is larger than that of water. Thus, the IL-rich phase is always the lower phase in contrast to n-alkane systems. In other words, $\underline{2}$ ($\bar{2}$) in the present IL-system equals $\bar{2}$ ($\underline{2}$) in n-alkane systems.

Characteristic parameters (γ_0, T_0, $\tilde{\gamma}$, $\tilde{T}$, $\Delta\gamma$, ΔT) of the fish-shaped phase diagrams are compiled in Table 1. The coordinates of the so-called fish head (lowest surfactant concentration at which a third middle phase appears) are γ_0 and T_0, whereas those of the fish tail (lowest surfactant concentration at which one phase is formed) are $\tilde{\gamma}$ and $\tilde{T}$, respectively. For the sake of

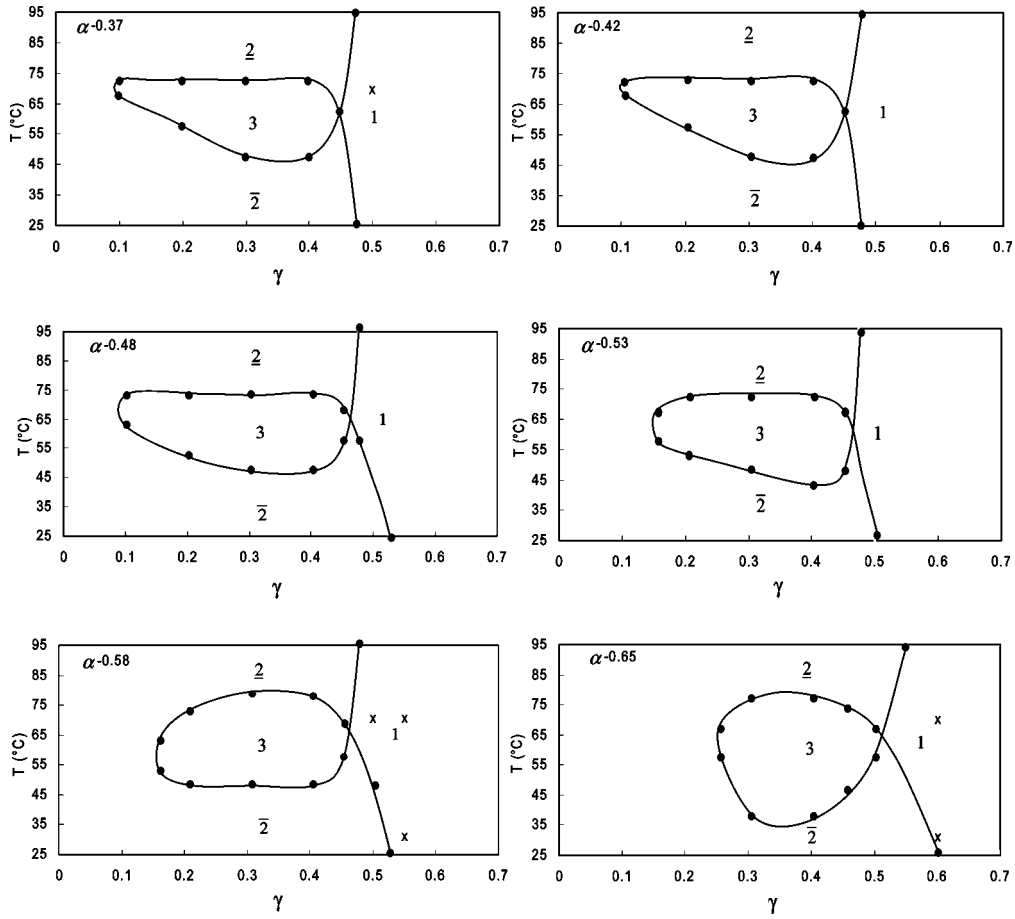

Figure 1. Fish-shaped phase diagrams (T-γ section) of the ternary system water/bmimPF$_6$/TX-100 at different IL/(IL + water) ratios α (α = 0.58 corresponds to equal volumes of H_2O and IL). T represents the temperature and γ is the mass fractions of surfactant. 1, $\underline{2}$, $\bar{2}$, and 3 correspond one phase, two phase (W/IL droplet μE), two phase (IL/W droplet μE), and three phase regions, respectively. The crosses locate the samples studied by SANS.

TABLE 1: Characteristic Parameters of the Measured Phase Diagrams[a]

α	Φ	γ_0	T_0/°C	$\tilde{\gamma}$	$\tilde{T}$/°C	$\Delta\gamma$	ΔT/°C
0.37	0.30	0.09	73.0	0.450	63.0	0.360	29.0
0.42	0.35	0.08	71.0	0.450	63.0	0.370	29.0
0.48	0.40	0.08	69.0	0.460	65.0	0.380	27.0
0.53	0.45	0.14	62.0	0.460	62.0	0.320	32.9
0.58	0.50	0.14	59.0	0.460	65.1	0.320	32.9
0.65	0.58	0.24	56.0	0.515	65.1	0.275	45.0
±0.01	±0.01	±0.01	±2	±0.01	±2	±0.01	±2

[a] IL mass fraction α; IL volume fraction Φ; coordinates of fish head γ_0, T_0; coordinates of fish tail $\tilde{\gamma}$, $\tilde{T}$; maximum extension of surfactant concentration and temperature of the 3-phase body $\Delta\gamma$, ΔT. Note that α = 0.58 corresponds to equal volumes of water and IL.

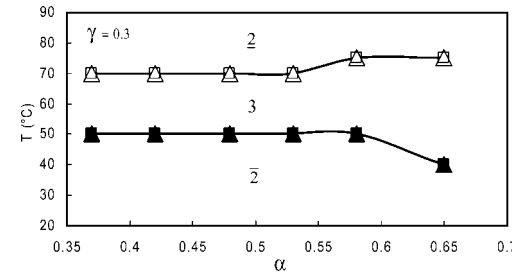

Figure 2. Shinoda cut (T-α section) of the ternary system water/bmimPF$_6$/TX-100 at a constant surfactant mass fraction γ = 0.3. Triangles: values taken from the fish shaped phase diagrams of Figure 1 (Δ: 3 to $\underline{2}$ and ▲: $\bar{2}$ to 3 transition). Squares: values measured independently at γ = 0.3 (□: 3 to $\underline{2}$ and ■: $\bar{2}$ to 3 transition).

completeness, the maximum extension of the γ-range ($\Delta\gamma$) and the T-range (ΔT) are also listed.

We checked the accuracy of the phase boundaries shown in Figure 1 by measuring the $\bar{2}$−3 and the 3−$\underline{2}$ phase transitions at a constant surfactant fraction γ as a function of the temperature T and the IL mass fraction α. For that purpose, we prepared two solutions, namely, (A) water + TX-100 with γ = 0.3 and (B) IL + TX-100 with γ = 0.3. We mixed these two solutions to obtain the same α as those shown in Figure 1. The resulting T-α representation, also called Shinoda cut, is shown in Figure 2 together with the results obtained via the first procedure at fixed α and varying γ. We found the same temperature for the $\bar{2}$ to 3 and for the 3 to $\underline{2}$ transitions, respectively, which demonstrates the accuracy of our measurements.

As is seen in Figure 1 and Table 1, the fish head is shifted toward higher γ and lower T values with increasing α. The reason for this shift is the high monomeric solubility of TX-100 in the IL. The more IL in the system, the more TX-100 is needed to saturate the IL-phase with monomers, which, in turn, leads to an increase in γ_0. The decrease in T_0 is due to the fact that with increasing IL content the tendency to form W/IL droplets increases. In other words, a change of the curvature from positive to negative values via an average zero mean curvature takes place at a lower temperature.[27] Comparison of these results with those obtained for the system water/*n*-dodecane/C_4E_1[28] reveals that there is one similarity and one difference. What is similar is the change of T_0 that decreases with increasing α, indicating the inclination to form negatively

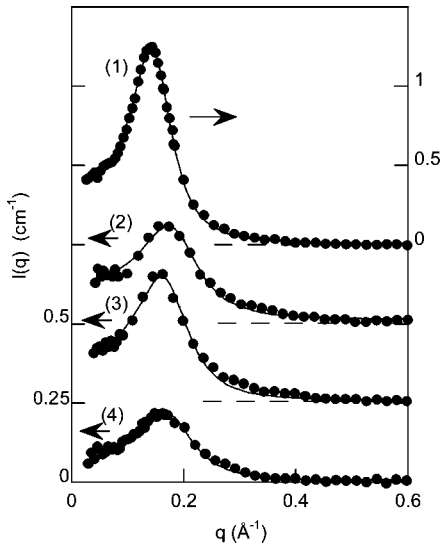

Figure 3. SANS spectra of TX-100 microemulsions at (α, γ) = (0.37, 0.5), (0.58, 0.50), (0.58, 0.54), and (0.65, 0.60), (curves 1−4, respectively). Curves 2 and 3 were shifted vertically for clarity. Symbols are the experimental data, and solid lines are TS fits.

curved interfacial layers at lower temperatures. What is different is the value of γ_0, which does not vary significantly with increasing α for the system water/*n*-dodecane/C_4E_1. The reason for this is the high monomeric solubility of C_4E_1 in both water and *n*-dodecane.

Looking at the coordinates of the fish tail, one sees that they are only slightly affected by a change of α. This is the only significant difference between the present IL and classical *n*-alkane μE. For the latter, $\tilde{\gamma}$ runs through a maximum around $\alpha = 0.4$, whereas $\tilde{T}$ increases continuously with α.[28,29] We expected a similar tendency for the present system and have no explanation yet as to why this has not been observed. Comparing the absolute $\tilde{\gamma}$ values of the systems water/bmimPF$_6$/TX-100 and water/*n*-dodecane/C_4E_1, one sees that both are equally inefficient. In both cases surfactant concentrations of ~50% are needed to solubilize water and the apolar phase. It is well-known for water/*n*-alkane/C_iE_j systems that the efficiency of a μE increases with increasing surfactant alkyl chain length.[22] The same general trend has been observed only recently for μE containing an IL (EAN) as the polar phase[16] and *n*-alkanes as the apolar phase. However, in both cases the increased efficiency is limited by the formation of a liquid crystalline lamellar phase (L_α) that extends and finally suppresses the 1-phase μE.[16,22] For example, no L_α phase was found in the system EAN/*n*-dodecane/$C_{12}E_4$, whereas it occurred in EAN/*n*-dodecane/$C_{14}E_4$, and completely dominates the 1-phase region in EAN/*n*-dodecane/$C_{16}E_4$.[16]

To get more insights into the microstructure of the water/IL/TX-100 microemulsions SANS measurements were carried out in the 1-phase region using deuterated water to enhance the contrast between the microdomains of the microemulsions (so-called bulk contrast). Typical SANS spectra of two nearly symmetric (equal solvent volume fractions) and two asymmetric (unequal solvent volume fractions) D_2O/IL/TX-100 μE are shown in Figure 3. The samples investigated by SANS are identified by a cross (×) in the phase diagrams shown in Figure 1. The data presented in Figure 3 were measured at $T = 69$ °C, which is very close to the measured $\tilde{X}$ point in the H_2O/IL mixture, so the microemulsion was expected to be bicontinuous. The preparation of samples in D_2O instead of H_2O was not expected to have a huge impact on the phase behavior, except for a small shift of the phase boundaries to lower temperatures.[30,31] We performed a temperature sweep at a few surfactant concentrations in D_2O and IL to ensure that the phase boundaries were not significantly affected, which indeed was the case. SANS measurements showed that the scattering intensities of 1-phase samples studied at $T = 31$ and 69 °C always consisted of a single broad correlation peak located in the q range between 0.12 and 0.17 Å^{-1}. Moreover, the asymptotic evolution in the high q domain showed that $I(q)$ decreases as q^{-4}, representing the Porod regime and demonstrating that the surfactant molecules form a well-defined interface between the two solvents in the corresponding short length scale ($\sim 1/q$).[32] The evolution of the scattering intensities is in agreement with SANS spectra usually observed for bicontinuous water/oil microemulsions close to the fish tail point in the 1-phase region. The broad correlation peak observed at $T = 69$ °C, as well as the similar scattering behavior observed near room temperature in the 1-phase domain indicates the formation of disordered microemulsions and excludes the existence of any lamellar structure. This confirms the results obtained by polarizing microscopy, with which no birefringence was detected between RT and 90 °C.

TABLE 2: Characteristic Structural Parameters in the 1-Phase Region at 69 °C near the $\tilde{X}$ Point[a]

T/°C	α	γ	ξ_{TS} / Å	d_{TS} / Å	$b/(4ac)^{1/2}$
69	0.37	0.50	23	43	−0.84
69	0.58	0.50	16	36	−0.79
69	0.58	0.54	17	37	−0.80
69	0.65	0.60	16	36	−0.78

[a] The ratio $b/(4ac)^{1/2}$ (eq 3) is the amphiphilicity factor.

For a more detailed analysis of the SANS spectra we first calculated the volume fraction of the two μE domains Φ_1 and Φ_2 as well as the corresponding scattering length densities ρ_1 and ρ_2. For calculating Φ_1 and Φ_2, we incorporated the hydrated ethylene oxide headgroup in the water phase and the alkyl tail into the IL phase. Second, we used the Teubner−Strey (TS) model to analyze the scattering intensities because this model was shown to adequately describe the structure of microemulsions.[33] According to this model, the neutron scattering intensity is given by eq 3,

$$I(q) = \Phi_1\Phi_2(\rho_1 - \rho_2)^2 \frac{1}{a + bq^2 + cq^4} \qquad (3)$$

where a, b, and c are related to two structural lengths in the microemulsion, namely, the mean repeat distance d_{TS} and the correlation length ξ_{TS}. The solid lines shown in Figure 3 are fits to eq 3. The d_{TS} and ξ_{TS} parameters extracted from the fit are displayed in Table 2. The agreement between the model and the experimental data is excellent. The TS model led to different length scales ($36 \le d_{TS} \le 43$ Å^{-1} and $16 \le \xi_{TS} \le 23$ Å^{-1}) depending on the sample composition. The small values of d_{TS} and ξ_{TS} reflect the low efficiency of this water/IL mixture. Because of the high surfactant concentration, a large interfacial area and thus small water- and IL-domains are formed. The amphiphilicity factor is shown in Table 2. This factor reveals that although the efficiency is low, its value, very close to −1, is a signature of strong amphiphiles.[34]

Comparison of TX-100 with $C_{12}E_6$ and $C_{14}E_4$. To increase the efficiency of the water/IL μE we exchanged TX-100 with more hydrophobic surfactants, namely, the monodisperse nonionic surfactants $C_{12}E_6$ and $C_{14}E_4$, respectively. The phase

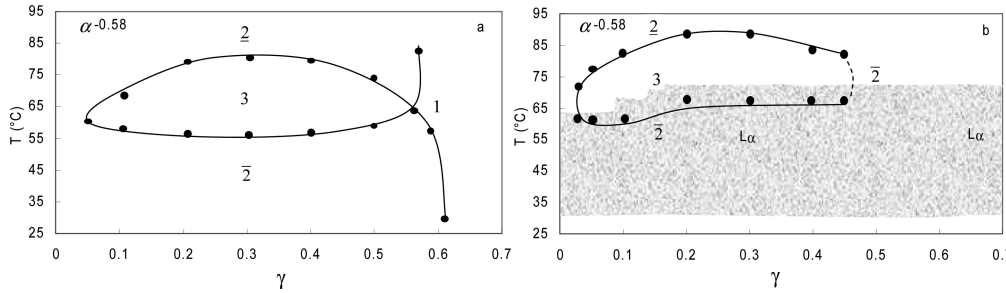

Figure 4. Fish-shaped phase diagrams (T-γ section) of the ternary system at $\alpha = 0.58$, (a) water/bmimPF$_6$/C_{12} E_6 and (b) water/bmimPF$_6$/$C_{14}E_4$. The chosen IL mass fraction α corresponds to equal volumes of water and IL. 1, 2, 2̄, and 3 correspond one phase, two phase (W/IL droplet μE), two phase (IL/W droplet μE), and three phase regions respectively. The gray region in panel b shows lamellar phase L_α.

behavior of the corresponding μE were studied at $\alpha = 0.58$ (corresponding to equal volumes of water and IL) and compared with those of IL/*n*-alkane/C_iE_j and water/*n*-alkane/C_iE_j systems. For the latter systems it is known that increasing the length of the hydrophobic chain significantly increases the surfactant efficiency and thus shifts the position of the $\tilde{X}$ point to lower surfactant concentrations and temperatures.[16,22]

The phase diagrams of symmetric water/bmimPF$_6$/$C_{12}E_6$ and water/bmimPF$_6$/$C_{12}E_4$ systems are presented in Figures 4a and 4b respectively. The longer alkyl chain length of $C_{12}E_6$ compared to TX-100 (C_8) shifts the position of the fish head to lower γ values (Figure 4a). This result is in agreement with data on IL/*n*-alkane and water/*n*-alkane systems. Further increasing the surfactant alkyl chain from C_{12} to C_{14} again shifts the fish head toward much lower γ values, as is shown in Figure 4b. However, in both cases, more surfactant is needed in order to form a 1-phase μE in water/bmimPF$_6$. This behavior conflicts with the results observed in water/*n*-alkane[22] and more recently in IL/*n*-alkane[16] systems. It is also noticeable that the increase in the alkyl chain length has only minor effects on ΔT, whereas it increases considerably $\Delta\gamma$. In the respective ternary water/*n*-alkane/C_iE_j systems, both ΔT and $\Delta\gamma$ shrink with increasing chain length. The solvophobicity of these alkyl oligoethyleneoxide surfactants in bmimPF$_6$ is certainly an explanation. It was argued that this IL acts as hydrogen-bond acceptor or donor and interacts mainly with solutes with either accepting or donating sites.[35] As alkyl chains do not have hydrogen bond acceptor and donor sites, its affinity toward the IL is thus limited. On the other hand, the polarity of this IL is relatively large and compares more with methanol or acetonitrile than with *n*-alkanes.[36,37] As a consequence, the solvophobicity of C_iE_j surfactants in bmimPF$_6$ is much certainly relatively higher than in water, thus the amphiphiles prefer water rather than the IL and therefore the relatively large extent of the 2̄ region or Winsor I domain observed in these ternary μE.

It is worth adding that due to the high solvophobicity of $C_{14}E_4$ in IL we have experienced some difficulties in determining the phase boundaries of the ternary system water/bmimPF$_6$/$C_{14}E_4$. Similar experimental problems were pointed out in ref 16. The shaded area in the corresponding phase diagram (Figure 4b) shows the region where the localization of phase boundaries was deterred by the occurrence of sample turbidity. These difficulties were exacerbated by the appearance of the L_α phase, which was characterized by optical microscopy. It was found that the lamellar domain extends up to $\gamma = 0.7$ between RT and 70 °C and dominates the phase diagram, preventing in this the exact localization of the $\tilde{X}$ point coordinates.

Conclusion

The ternary phase behavior of microemulsions consisting of water, the hydrophobic ionic liquid bmimPF$_6$ and the nonionic surfactant TX-100 was studied as a function of temperature and surfactant concentration at different ionic liquid mass fractions. The microstructure of some selected monophasic samples were also investigated by SANS and polarizing microscopy at different temperatures and confirmed the presence of bicontinuous microemulsions. A lamellar phase was not observed in the 1-phase region of TX-100 microemulsions. The coordinates of the $\tilde{X}$ points in this system stay nearly constant over the entire studied α-range, where only a slight increase of $\tilde{\gamma}$ with IL content has been observed. Very high $\tilde{\gamma}$ values have been measured, indicating a low efficiency of TX-100. These large $\tilde{\gamma}$ values are reflected in the measured short length scales of the microemulsions, that is, short mean repeat distances and correlation lengths. The fish-shaped three-phase region is distorted at low and high α values, whereas it has a symmetric form at intermediate values of α.

These observations are qualitatively similar to the classical water/*n*-alkane/C_iE_j[22,28] and to the novel IL/*n*-alkane/C_iE_j μE.[16] As far as the efficiency is concerned, a comparison of C_iE_j with TX-100 μE shows that the water/bmimPF$_6$ system gets less efficient with increasing chain length. An explanation could be the solvophobicity of IL toward increasing alkyl chain length of the surfactant. These findings are in agreement with recent investigations of the liquid−liquid phase diagrams for mixtures of bmimPF$_6$ and *n*-alkanes, where it was shown that the temperature of the miscibility gap increases with increasing the length of the hydrocarbon alkyl chain.[35] Our results show that the knowledge gained from the classical water/oil/C_iE_j systems cannot be transferred straightforwardly to aqueous μE containing hydrophobic ionic liquids, that is, previous concepts for formulating and characterizing μE must be studied in more detail. For example, the low efficiency of the TX-100 μE cannot be enhanced by increasing the hydrophobicity of the surfactant. A thorough investigation of IL interactions with nonionic surfactants is needed in order to enhance the efficiency of IL-containing μE and to promote their use in various applications.

Acknowledgment. The authors thank Professor R. Strey for fruitful discussions while carrying out the experimental work. Financial support of this research study by Centre National de la Recherche Scientifique (CNRS) is gratefully acknowledged. We acknowledge the support of the CNRS/CEA joint Léon Brillouin laboratory in providing the neutron facilities used in this work. We thank Dr. A. Lapp and Dr. S. Asnacios for providing assistance with the SANS and the optical microscopy measurements respectively. C. S. thanks the French−Irish exchange program Ulysses and the Marie Curie Research Training Network "Self-Organization under Confinement" (SOCON, contract No. MRTN-CT-2004-512331) for financially supporting her two-month stay in Paris in 2007.

References and Notes

(1) Welton, T. *Chem. Rev.* **1999**, *99*, 2071.
(2) Holbrey, J. D.; Seddon, K. R. *Clean Prod. Proc.* **1999**, *1*, 223.
(3) Law, G.; Watson, P. R. *Langmuir* **2001**, *17*, 6138.
(4) Kristin, A. F.; Panday, S. *Langmuir* **2004**, *20*, 33.
(5) Akle, B. J.; Bennett, M. D.; Leo, D. J. *Sens. Actuators A* **2006**, *126*, 173.
(6) Zhang, Y.; Shen, Y.; Li, J.; Niu, L.; Dong, S.; Ivaska, A. *Langmuir* **2005**, *21*, 4797.
(7) Alvaro, M.; Carbonell, E.; Ferrer, B.; Garcia, H.; Herance, J. R. *Photochem. Photobio.* **2006**, *82*, 185.
(8) Matsumoto, M.; Inomoto, Y.; Kondo, K. *J. Membr. Sci.* **2005**, *246*, 77.
(9) Nakashima, T.; Kimizuka, N. *J. Am. Chem. Soc.* **2003**, *125*, 6386.
(10) Holbrey, J. D.; Seddon, K. R. *J. Chem. Soc., Dalton Trans.* **1999**, 2133.
(11) Anthony, J. L.; Magginn, E. J.; Brennecke, J. F. *J. Phys. Chem. B* **2001**, *105*, 10942.
(12) Dzyuba, S. V.; Bartsch, R. A. *Chem. Phys. Chem.* **2002**, *3*, 161.
(13) Gao, Y.; Li, N.; Zheng, L.; Zhao, X.; Zhang, J.; Cao, Q.; Zhao, M.; Li, Z.; Zhang, G. *Chem.—Eur. J.* **2007**, *13*, 2661.
(14) Gao, Y.; Han, S.; Han, B.; Li, G.; Shen, D.; Li, Z.; Du, J.; Hou, W.; Zhang, G. *Langmuir* **2005**, *21*, 5681.
(15) Eastoe, J.; Gold, S.; Rogers, S. E.; Paul, A.; Welton, T.; Heenan, R. K.; Grillo, I. *J. Am. Chem. Soc.* **2005**, *127*, 7302.
(16) Atkin, R.; Warr, G. G. *J. Phys. Chem. B* **2007**, *111*, 9309.
(17) Gao, H. X.; Li, J. C.; Han, B. X.; Chen, W. N.; Zhang, J. L.; Zhang, R.; Yan, D. D. *Phys. Chem. Chem. Phys.* **2004**, *6*, 2914.
(18) Kahlweit, M.; Strey, R. *Angew. Chem. Int. Edn. Engl.* **1985**, *24*, 654.
(19) Kahlweit, M.; Strey, R.; Firman, P.; Haase, D.; Jen, J.; Schomäcker, R. *Langmuir* **1988**, *4*, 499.
(20) Kahlweit, M.; Strey, R.; Firman, P. *J. Phys. Chem.* **1986**, *90*, 671.
(21) Kahlweit, M.; Strey, R.; Busse, G. *J. Phys. Chem.* **1990**, *94*, 3881.
(22) Sottmann, T.; Strey, R. In *Soft Colloids V—Fundamentals in Interface and Colloid Science*; Lyklema, J. Ed.; Elsevier: Amsterdam, 2005; Ch. 5.
(23) Seth, D.; Chakraborty, A.; Setua, P.; Sarkar, N. *Langmuir* **2006**, *22*, 7786.
(24) Seth, D.; Chakraborty, A.; Setua, P.; Sarkar, N. *J. Chem. Phys.* **2007**, *126*, 224512.
(25) Gao, Y.; Li, N.; Zheng, L.; Zhao, X.; Zhang, S.; Han, B.; Hou, W.; Li, G. *Green Chem.* **2006**, *8*, 43.
(26) Dupont, J.; Consorti, C. S.; Suarez, P. A. Z.; de Souza, R. F. *Org. Synth.* **2002**, *79*, 236.
(27) At the fish head, the first droplet of the middle phase is formed. In the water/*n*-alkane/C_iE_j system with equal water and oil volume fractions, the temperature at the fish head and tail are the same, which, in turn, means that the microstructure is the same. Increasing γ simply increases the volume of the middle phase without altering the bicontinuous structure.
(28) Burauer, S.; Sachert, T.; Sottmann, T.; Strey, R. *Phys. Chem. Chem. Phys.* **1999**, *1*, 4299.
(29) Burauer, S.; Belkoura, L.; Stubenrauch, C.; Strey, R. *Coll. Surf. A: Physicochem. Eng. Aspects* **2003**, *228*, 159.
(30) Strey, R.; Glatter, O.; Schubert, K. V.; Kaler, E. W. *J. Chem. Phys.* **1996**, *105*, 1175.
(31) Stubenrauch, C.; Frank, C. H.; Strey, R.; Schmidt, C. *Langmuir* **2002**, *18*, 5027.
(32) Porod, G. In *Small Angle X-ray Scattering* Glatter, O., Kratky, O. Eds.; Academic Press: London, 1982.
(33) Teubner, M.; Strey, R. *J. Chem. Phys.* **1987**, *87*, 3195.
(34) Schubert, K. V.; Strey, R. *J. Chem. Phys.* **1991**, *95*, 8532.
(35) Domańska, U.; Marciniak, A. *J. Chem. Eng. Data* **2003**, *48*, 451.
(36) Reichardt, C. *Green Chem.* **2005**, *7*, 339.
(37) Aki, S. N. V. K.; Brennecke, J. F.; Samanta, A. *Chem. Commun.* **2001**, 413.

JP808643S